RESEARCH PAPER

Renewable Dragon Fruit Peel Extract-Based Magnesium Oxide Nanoparticle Synthesis and Burn-Related Pseudomonas Aeruginosa Antibacterial and Antioxidant Features

*Zahra Falih Mahdi, Huda Jasim M. Altameme *, Nisreen Kaddim Radi*

Biology Department, College of Science for Women, University of Babylon, Babylon, Iraq

ARTICLE INFO

Article History:
Received 10 March 2026
Accepted 17 May 2026
Published 01 July 2026

Keywords:
Biological activity
Burn infection
Cactaceae
Hylocereus polyrhizus
MgO NPs

ABSTRACT

The current work intended to establish an ecologically friendly method for the manufacture of magnesium oxide nanoparticles (MgO NPs) utilizing *Hylocereus polyrhizus* (dragon fruit) peel aqueous extract and assess their biological potential. Initial phytochemical screening found flavonoids, phenolics, tannins, alkaloids, and saponins in the plant extract, suggesting its potential as a natural reducing and stabilizing agent. In the present study, UV-visible spectroscopy (UV-Vis), atomic force microscopy (AFM), field-emission scanning electron microscopy (FE-SEM), X-ray diffraction (XRD), and Fourier-transform infrared spectroscopy (FTIR) were used to characterize our biosynthesized magnesium oxide nanoparticles. It was found that we have formed nanoparticles that are mainly spherical and display a nanoscale size distribution. Our work revealed that the synthesized nanoparticles have a dose-dependent antioxidant effect in the DPPH radical scavenging assay, achieving 59.33% at a concentration of 1 mg/mL, and also examined their response to multidrug-resistant burn infections caused by *Pseudomonas aeruginosa*. Increasing the nanoparticle concentration resulted in larger inhibitory zones, indicating their potential action. Results of biocompatibility testing indicated that the magnesium oxide nanoparticles we synthesized exhibited no hemolytic activity at any of the doses tested, demonstrating excellent biomedical safety. Our work indicates that magnesium oxide nanoparticles, synthesized from dragon fruit peel extract using green methods, exhibit significant antioxidant and antibacterial properties, potentially offering a novel approach to treating burn-infected wounds caused by resistant bacterial strains.

How to cite this article
Falih Mahdi Z., M. Altameme H., Kaddim Radi N. Renewable Dragon Fruit Peel Extract-Based Magnesium Oxide Nanoparticle Synthesis and Burn-Related Pseudomonas Aeruginosa Antibacterial and Antioxidant Features. J Nanostruct, 2026; 16(3):3323-3336. DOI: 10.22052/JNS.2026.03.026

INTRODUCTION

In the present healthcare setting, which is to a great degree based on traditional and herbal medicine, the latter still plays a large role. It is reported that natural products do better in terms of safety and performance as compared to their synthetic counterparts [1]. Also, we are seeing a recent increase in interest in using herbal plants as a medical resource due to their natural makeup, availability in local areas, low cost, easy administration, and potentially fewer side effects [2]. Treating burn wounds remains a challenge

* Corresponding Author Email: wsci.huda.j@uobabylon.edu.iq

for modern medicine, especially in developing countries that cannot afford expensive, advanced therapies. Therefore, treating burn wounds remains a challenging task, particularly in terms of cost-effective therapy [3, 4]. In the clinical trials mentioned, some herbal remedies are more effective than standard treatments for burn wounds. They speed up healing and lower inflammation. The growing interest in alternative medicine and herbal medicine encourages further research [5].

Hylocereus (pitahaya, or dragon fruit) is a Cactaceae genus of climbing plants with aerial roots that produce glabrous berries with enormous scales [6]. Over ten countries grow the dragon fruit plant for commercial purposes due to its exceptional drought tolerance, fruit yield, and economic value. Southern Mexico, Guatemala, and Costa Rica introduced dragon fruit to the tropical nations of South Asia in 1990 [7]. [8] divided *Hylocereus* based on the physical characteristics of the fruit into five major types, and one of the types under study is *Hylocereus polyrhizus*, which is a fruit with a pink peel and a red pulp inside.

Dragon fruit is one fruit linked to a reduced risk of chronic illnesses [9, 10]. In fact, it is a source

Fig.1. Sample collection of dragon fruit (A- Whole fruit of dragon; B- Peels of dragon; and C and D- Stages of drying, E- Fine powder of peels).

Table 1. The phytochemical screening in dragon peel extract.

Components	Reagent	Positive results	References
Glycosides	Benedict's test	appearance of a red precipitate	[18]
Terpenes	Salkowski Test	appearance of a reddish-brown layer	[19]
Tannins	Ferric Chloride test	appearance of a bluish-green	[18]
Flavonoids	Concentrated Sulfuric Acid test	appearance of a dark yellow	[20]
Alkaloids	Mayer test	The presence of turbidity	[21]
Phenolic	Ferric Chloride test	appearance of a bluish-green	[21]
Saponins	Fast stirring	Continued foam formation	[22]

of bioactive compounds that provide health benefits such as antidiabetic, anti-inflammatory, antioxidant, anticancer, and antibacterial properties. Furthermore, it sees a global increase in its consumption, which is a result of these positive health effects [11]. Pitahaya peel reports that it has a large amount of health benefits from its high content of betacyanin, which is an antioxidant and an antibacterial agent. Also, it contains other pigments that may be used as food colorants or preservatives [12]. Furthermore, in the past 10 years, there has been an increase in the use of metals and metal nanoparticles, which are used for infection fighting [13]. Metal NPs are the main options for wound dressing development because of their antibacterial capabilities and low toxicity [14]. Additionally, nanofibers are generally used with the integration of synthetic or natural polymers in wound repair approaches because of their bioactivity and biodegradability characteristics [15], possessing advantages like antibacterial properties and providing a moist environment [16]. Hence, this study aimed to preliminarily assess the efficacy of magnesium oxide nanoparticles synthesized using dragon fruit peel against *Pseudomonas aeruginosa* burn infections and to confirm the antioxidant and biodegradability of the extract, with the goal of obtaining an environmentally friendly nanomaterial derived from plant peels for treating burn inflammation as an alternative to pharmaceuticals.

MATERIALS AND METHOD

Production of aqueous extract from the peel of the plant

An aqueous extract was generated from dragon fruit (*Hylocereus polyrhizus*) peels using a maceration technique [17]. About 20 gm of the pulverized plant extract was dissolved in 1000 mL of distilled water. The mixture was continuously agitated using a magnetic stirrer at approximately 700 rpm and maintained at a temperature of 37 °C for 24 hours. Following the extraction period, the mixture was filtered using Whatman No. 1 filter paper and then centrifuged at 4500 rpm for 30 minutes. The supernatant containing the suspended active bio-compounds was carefully collected and then used for the subsequent preliminary chemical detection and Nano biosynthesis process (Fig. 1).

Preliminary chemical detection of active compounds in dragon peel extract

The phytochemical analysis of the plant extract was conducted using standard methods. Specifically, the extract was screened for phytochemicals (glycosides, alkaloids, flavonoids, tannins, terpenoids, and saponins), as explained in Table 1, which lists the compounds to be detected, the name of the test, the positive result for each test, and the references used in its preparation.

Synthesis of magnesium oxide nanoparticles with dragon fruit peel extract

To synthesize magnesium oxide nanoparticles (MgO NPs), three grams of magnesium oxide precursor (Mg $(NO_3)_2$) were added to 1000 mL of the prepared dragon fruit peel aqueous extract, which acts as a natural bio-reducing and capping agent. The reaction mixture was put in the shaker incubator and made to undergo 24 hours of continuous agitation, which in turn ensured uniform mixing and interaction between plant

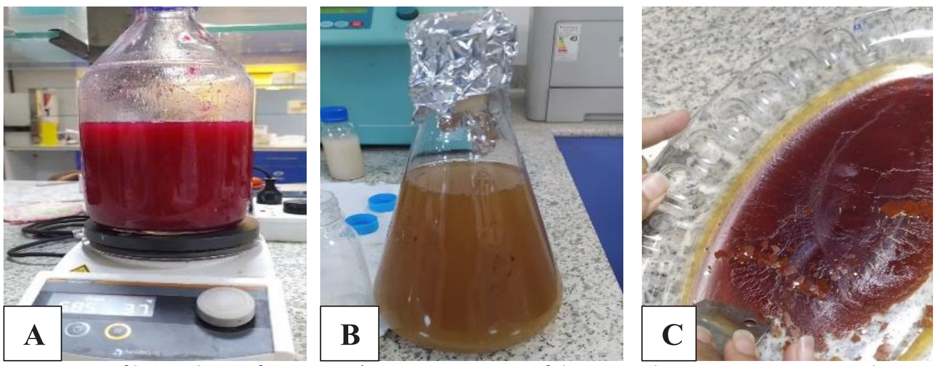

Fig. 2. Steps of biosynthesis of MgO NPs. (A- aqueous extract of dragon peels, B- aqueous extract with MgO, and C- MgO NPs after drying).

phytochemicals and the magnesium precursor. Afterwards, the suspension was poured into a wide dish and transferred to a drying incubator for an additional 24 hours to facilitate complete solvent evaporation. Finally, the resulting dried material was manually scraped, collected, and thoroughly ground into a fine nano powder for further physical and biological characterizations (Fig. 2).

Synthesized MgO-NPs description

Physical and biological characterization are the most common methods for determining the properties of nanoparticles:

UV/Vis Spectroscopy Analysis: NPs' UV and visible spectra were regularly characterized using a UV-1800 spectrophotometer (Shimadzu, Japan). The sample's absorption spectrum was 250–280 nm. The instrument was zeroed with distilled water 24 hours after preparation [23].

Atomic Force Microscopy: Nanomaterial dispersion, aggregation, size, and form are studied using atomic force microscopy (AFM). An AFM probe at one end of a spring-like cantilever interacts with the material. The material-tip interaction creates attractive or repulsive forces. Such pressures reveal the sample's topography [24].

Field Emission Scanning Electron Microscopy Analysis: The achieved nanoparticles' size, shape, and phenotypic characteristics were measured using the FE-SEM, SIGMA VP-500, and ZEISS high-efficiency scanning electron microscope [22].

X-Ray Diffraction Analysis: To analyze nanoparticle structure, X-ray diffraction (XRD-6000, Shimadzu, Japan) is used. The equipment used a Cu (kα) radiation source with a λ = 1.5405 Å wavelength, 60 kV voltage, 80 mA current, and 5°/min scanning speed (from 20° to 80°). Measuring a dried sample using filter paper.

Fourier-transform infrared spectroscopy Analysis: FTIR was used to detect biomolecule functional groups on the plant extract surface and their possible role in nanoparticle formation. To make granules, the material was dried and combined with potassium bromide. We used a TENSOR 27 (Bruker Optik GmbH) for FTIR spectroscopy from 400 to 4000 cm^{-1}.

Antioxidant effect study

According to [25], the DPPH (2,2-diphenyl-1-picrylhydrazyl) test measured free radical scavenging ability. Sample solutions were prepared at various concentrations (0.125, 0.25, 0.5, and 1 mg/ml). A microplate was used to mix 100µl of freshly made DPPH solution in methanol with 100µl of the sample at different concentrations. To prevent light-induced reagent damage, the microplate was incubated in the dark for 30 minutes. After incubation, an ELISA reader assessed absorbance at 517 nm. DPPH radical scavenging activity was calculated using Eq. 1.

A_0 indicates control absorbance, whereas A_1 accounts for the tested sample's absorbance.

Antimicrobial Susceptibility Testing (AST)

Thirty isolates of resistant *Pseudomonas aeruginosa* were collected from burn patients in hospitals in Babylon Governorate. Bacterial identity was confirmed, and antibiotic susceptibility testing was performed using the Vitek 2 compact device. The manufacturer's guidelines for preparing the bacterial suspension were followed. A pre-prepared purified culture was transferred to a transparent test tube (12 × 75 mm) and suspended in 3.0 mL of sterile saline to establish a sufficient number of colonies. A Densi-Chek turbidity meter was used, set to 0.5 McFarland units. The same suspension was used to identify Gram-positive and Gram-negative bacteria using a Vitek 2 compact analyzer. The Vitek 2 chamber received the Gram-positive bacterial cassettes, with the sample suspension tubes placed at the end. The Vitek 2 compact analyzer showed that the isolate was sensitive to antibiotics [26].

Antibacterial effect study

MgO nanoparticles synthesized from dragon fruit peel extract were tested for antibacterial activity against burn infection-isolated *Pseudomonas aeruginosa* utilizing the well diffusion technique. We diluted MgO NPs at 250, 500, 750, and 1000 µg/ml. A 0.5 McFarland standard was applied to indicator bacteria active for 18 hours at 37°C.

$$\text{DPPH radical scavenging effect (\%)} = \frac{A0 - A1}{A0} \text{x } 100 \qquad (1)$$

Sterile nutrient agar plates were used to grow bacteria, and a sterilized cork borer cut wells. After applying 100µl of each extract concentration to wells, they were incubated at 37°C for 24 hours and assessed for inhibitory zones in mm. Note that the agar well diffusion method was used as a preliminary screening approach, and the minimum inhibitory concentration (MIC) and minimum lethal concentration (MBC) will be determined in subsequent experiments.

Study of the hemolysis impact

Hemolysis tests were conducted on three healthy donor's blood, following [27]. Blood samples were treated with 15µL of nanoparticles at doses of 0.12, 0.25, 0.5, and 1 mg/mL in Tyrode's solution per sample. The study employed Tyrode's solution as a negative control and Triton X-100 as a positive control in 285µL of blood. An incubator shaker incubated the suspension at 37°C for 4 hours. Once incubated, the suspension was centrifuged at 10,000 rpm for 5 minutes. At 550 nm, an ELISA reader examined the supernatant in a 96-well plate to assess hemolysis. It was determined using the hemolysis % equation (Eq. 2):

$$\text{Haemolysis}(\%) = \frac{(\text{OD550nm sample} - \text{OD550nm tyrode})}{(\text{OD550nm Triton X} - 100\ 1\% - \text{OD550nm tyrode})} \text{x } 100 \qquad (2)$$

RESULTS AND DISCUSSION

It is clear from this work that *Hylocereus polyrhizus* fruit peel extract is a viable source of various phytochemicals. The results indicate the extract tested positive for glycosides, terpenes, tannins, flavonoids, alkaloids, phenolics, and saponins, which we determined via standard procedures. Also, for these components, which are responsible for the bioactivity of a medicinal plant—that is, its therapeutic action—note that the extract has health benefits and shows antibacterial properties, as each group functions to do so. This study found some of the results to support what other studies have reported, which is that *Hylocereus polyrhizus* is a source of several phytochemicals, including glycosides, terpenes, tannins, flavonoids, alkaloids, phenolics, and saponins [28, 29], but did not see the same results as [30] and [31], who did not find evidence of alkaloids in their analysis of dragon fruit peels, which also had low levels of flavonoids and phenols and high levels of terpenoids. The discrepancies in our findings may be attributed to the utilization of varying extraction methods, solvents, and plant parts in the study [32]. The present study used crude extract directly, while other studies used different solvents that play an important role in increasing the solubility of some phytochemical compounds and decreasing the solubility of others, depending on the polarity of the solvents [33].

Dragon fruit peel secondary metabolites are affected by internal and external influences, which vary by growing area, according to [31]. Climate, geography, altitude, and morphological differences affect phytochemical types and concentrations, while genetic variation, growth stage, plant age, and organ used (e.g., peel, pulp, or seed) do. Diverse plant species and development phases have diverse biological routes, which affect their phytochemical makeup. Internal dynamics affect plant metabolic responses, which explain changes in extract composition [34].

Characteristic of the synthesized MgO-NPs

As particles were deposited throughout the production process of magnesium oxide nanoparticles, the color of the aqueous extract of dragon fruit peels changed from an initial red to a yellowish-brown suspension, and the consistency also altered. After being exposed to the magnesium precursor, the dragon fruit peel demonstrated its capacity to produce magnesium oxide nanoparticles via biosynthesis. The distinct color change of the reaction mixture after 24 hours of incubation in a shaking incubator is clear evidence of the formation of stable nanoparticles by a group of environmentally friendly reducing and capping agents (like phenols and alkaloids) present in the extract, which reduced the magnesium ions, as confirmed by [35]. According to the visual transition, the color change of the reaction mixture from red to yellowish-brown indicates the successful production of magnesium oxide nanoparticles.

UV-Visible spectroscopy was utilized to confirm the biosynthesis of MgO NPs using an extract from dragon fruit peels. As shown in Fig. 3, the synthesized nanoparticles exhibited a strong and sharp absorption peak in the UV region at 230 nm, reaching a high absorbance intensity of approximately 2.45. This characteristic peak at 230 nm is attributed to an absorption peak attributed to electronic transitions or band gap characteristics. The shift or position of the peak at this wavelength, 230 nm, indicates the successful reduction of magnesium ions and their stabilization by the phytochemicals (phenols and alkaloids) present in the extract. The spectrum in Fig. 3 also shows that the absorbance slowly drops off as it approaches closer to the visible range. This confirms that the biosynthesized MgO NPs are optically pure and that there are no large-scale aggregations.

Fig. 4 (A and B) shows the 2D atomic force microscopy (AFM) and the 3D representation of the MgO nanoparticles synthesized using the aqueous extract of dragon fruit peels, respectively. Based on the topographic analysis, the particle size ranged from 26.74 to 53.96 nm. The atomic force microscopy technique provides images that enable quantitative measurements of the material's surface, including the root-mean-square (RMS) roughness and surface roughness average, which confirm the nanoscale features and the high surface-to-volume ratio of the prepared particles. These morphological findings are in excellent agreement with [36], who reported that synthesized MgO nanoparticles exhibit a uniform spherical distribution

The present study looked at the morphology of synthesized magnesium oxide nanoparticles (MgO NPs) via FESEM. As depicted in the FE-SEM images (Fig. 5), the MgO NPs exhibit a predominantly spherical appearance with an estimated diameter range of 35.40–85.15 nm, showing a relatively homogeneous morphology. The larger particles or clusters observed in the micrograph (Fig. 5) may be a result of the unwanted aggregation that

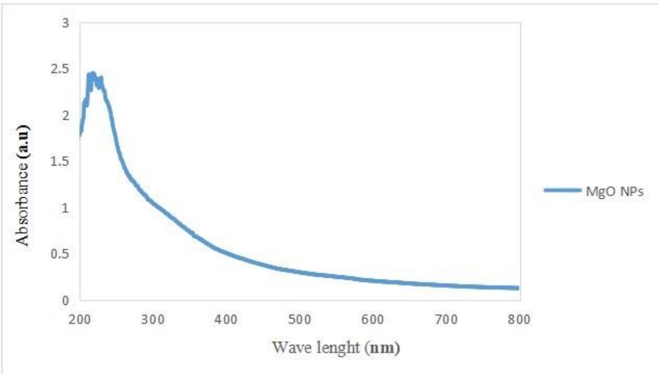

Fig. 3. UV-vis absorption spectrum of MgO nanoparticles synthesized by dragon fruit peel aqueous extract.

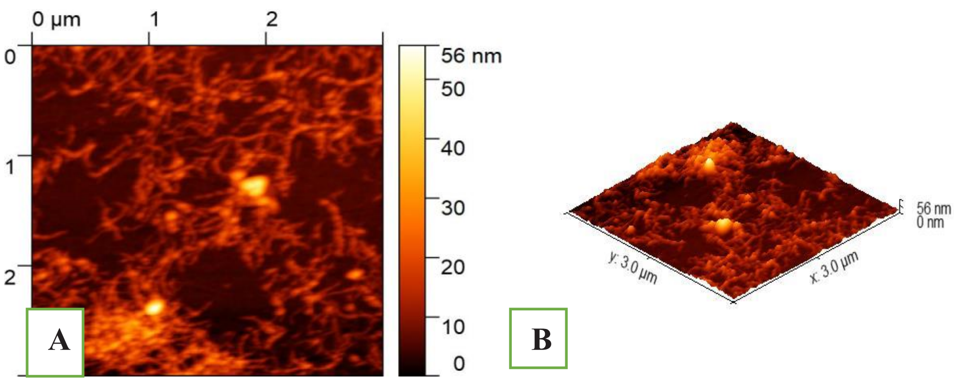

Fig. 4. The 2D (A) and 3D (B) AFM images of MgO nanoparticles synthesized by dragon fruit peel extract.

occurs throughout the drying process. As soon after evaporation as when it happens, particle concentration increases. That increase in ionic concentration, which results from evaporation, may in turn reduce electrostatic repulsion, which in turn causes agglomeration [36]. Also of great importance is the spherical shape and nanoscale size of the MgO NPs, which play a key role in their surface reactivity and biological effectiveness [37].

Our study found that materials synthesized from a magnesium precursor and dragon fruit peel aqueous extract have a high surface area nanocrystalline structure, as reported by X-ray diffraction analysis. Fig. 6 presents a very broad diffraction pattern with a main peak at 2θ ≈ 36.8°, characteristic of the material we are looking at, which is mostly of the cubic MgO phase. In this case, the X-axis (2θ) represents the diffraction angle, which is related to specific crystallographic planes in the crystal lattice, such as the (111) plane. The Y-axis (intensity) represents the X-ray diffraction intensity at each angle. Additionally, the large peak width is a result of very small crystallite sizes. This structural behavior and intensity variation we see is in agreement with what is reported in the literature for nanometer-sized MgO.

Fig. 7 indicates the peak values and functional groups for the biosynthesized magnesium oxide nanoparticles (MgO NPs) produced by dragon fruit peel extract. The X axis (wave number, cm^{-1}) displays the frequency of the infrared light, and the Y axis (% transmittance) indicates what

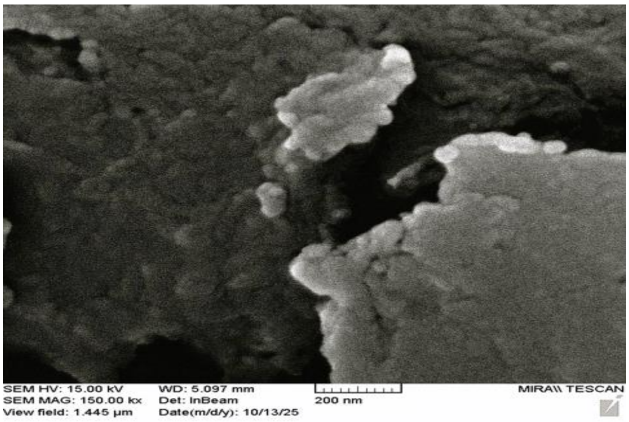

Fig. 5: Field Emission Scanning Electron Microscopy (FE-SEM) images showing the surface morphology of the biosynthesized MgO nanoparticles.

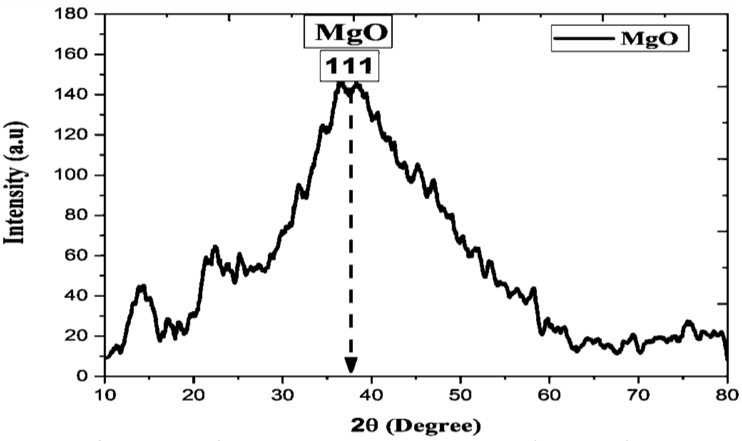

Fig. 6. Diffractogram of synthesized MgO nanoparticles (MgO NPs) showing a prominent broad peak at 2θ ≈ 36.8°.

percent of light is passing through the sample. In the FT-IR spectrum, the bioactive compounds, mainly phenols and alkaloids, are present and also function as dual reducing and capping agents. Furthermore, our IR spectrum shows the interaction of hydroxyl and carbonyl groups with magnesium ions, which in turn facilitates their reduction into MgO NPs. We see an intense peak at 3435 cm^{-1}, which is that of O-H stretching vibrations, and also a sharp one at 1619 cm^{-1}, which is due to C=C/C=O stretching. A peak was also observed at 665 cm^{-1}, a characteristic sign of Mg-O bond extension, confirming the crystalline structure of the metal oxide nanoparticles. This result is highly consistent with what [38] reported regarding magnesium oxide nanoparticles.

Biological applications of MgO nanoparticles

2,2-diphenyl-1-picrylhydrazyl (DPPH) free radical scavenging Assays were used to detect the antioxidant ability of the chemical MgO NPs, which were biosynthesized from the dragon fruit peel by reducing DPPH free radicals. The results displayed in the screening findings of Fig. 8 show that the biogenic MgO NPs from the dragon fruit peel effectively scavenged the DPPH radical. It also indicates that the percentage of scavenging goes down as the concentration of the nanoparticles goes down (from 59.335% at 1 mg/ml to 51.702% at 0.125 mg/ml), indicating a concentration-dependent enhancement in activity. DPPH tests are well-known for being able to tell how well a substance can work as an antioxidant. The idea behind the DPPH test is that the color of the DPPH solution shifts from purple to yellow when

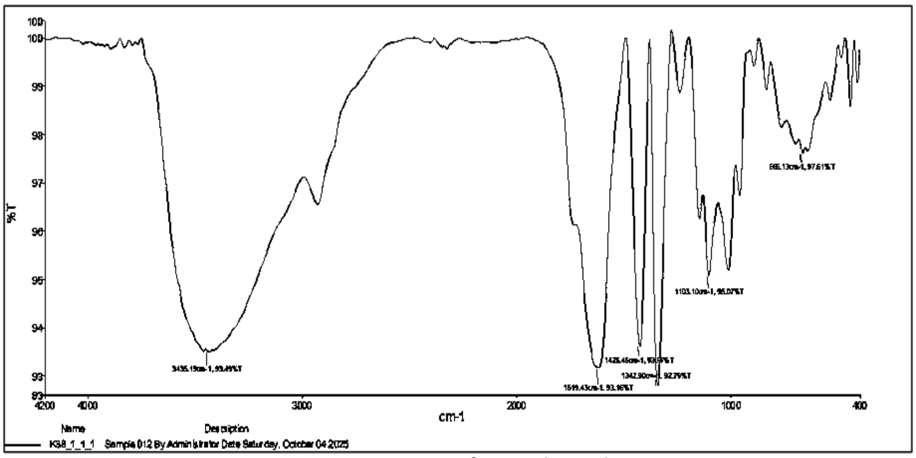

Fig. 7. FT-IR Spectra Pattern of Biosynthesized MgO NPs.

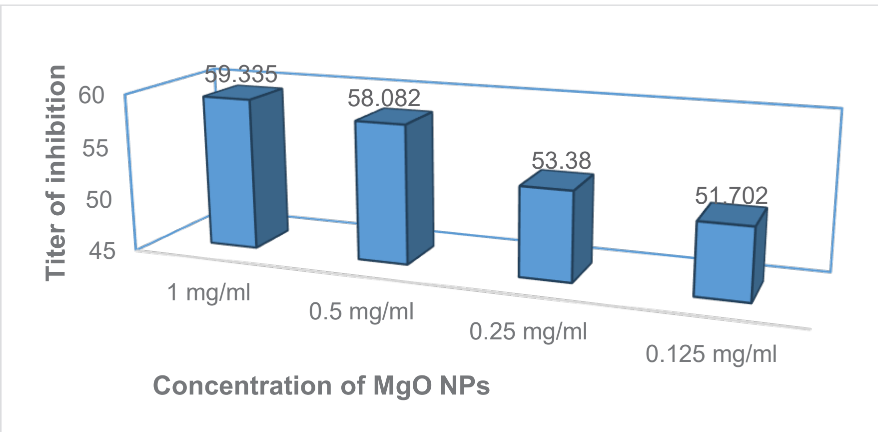

Fig. 8. DPPH free radical scavenging activity of biosynthesized MgO nanoparticles at various concentrations.

the antioxidant gets rid of radicals. Research reports that biosynthesized MgO NPs are good at what they do, which is act as antioxidants and also put a stop to DPPH radicals. Also seen in our study is that the antioxidant performance of the biosynthesized MgO NPs is great, which in turn presents them as a very effective source of antioxidants. Therefore, the biosynthesized MgO NPs are facilitated by the bio-capping of the aqueous plant extract phytochemicals [25], which act as free radical scavengers, transforming them into stable molecules. Researchers believe that the peel of the purple *Hylocereus* species has antioxidant properties because of its bright color [39].

The antimicrobial susceptibility testing of *P. aeruginosa* isolates recovered from burn wound cases in Babylon Province revealed a markedly high resistance profile across multiple antibiotic classes, indicating the presence of multidrug-resistant (MDR) strains. Complete resistance (100%) was recorded against both Ceftazoline and Ceftazidime, while resistance rates of 76%, 85%, 80%, 75%, 66%, 60%, and 50% were observed against Piperacillin, Ciprofloxacin, Gentamicin, Amikacin, Meropenem, Imipenem, and Cefepime, respectively (Fig. 9).

In terms of complete resistance (100%) to ceftazoline, that is what we expect, as P. aeruginosa has intrinsic resistance to first-generation cephalosporins, which is a result of their outer membrane structure and also from the expression of AmpC beta-lactamase in a constant state. Furthermore, it was found to have full resistance to ceftazidime (100%), which is very alarmingly high. This study's results are in line with those of [40], which found that more than 90% of burn patients had *P. aeruginosa* that was resistant to ceftazidime.

Our findings are consistent with a prior investigation, which found that 85% of *P. aeruginosa* isolates from burn patients were resistant to ciprofloxacin [41]. The overprescription of ciprofloxacin in healthcare settings is a major contributor to the rise of fluoroquinolone resistance. A correlation between the two was shown to be statistically significant, according to [42]. Also noteworthy were the resistance rates to aminoglycosides; 80% of cases showed resistance to gentamicin and 75% to amikacin. An extensive study conducted at burn centers found that 90% of P. aeruginosa isolates were resistant to amikacin and 98% to gentamicin [41]. This indicates that burn-associated *P. aeruginosa* is a global problem that is becoming worse.

In this study, carbapenem resistance was seen as a large issue, which was noted in meropenem at 66% and in imipenem at 60%. Furthermore, the most common beta-lactamase genes, blaTEM, blaVIM, and blaCTX-M, were found in 40% of *P. aeruginosa* isolates from burn wounds [43]. Increased carbapenem resistance in our study

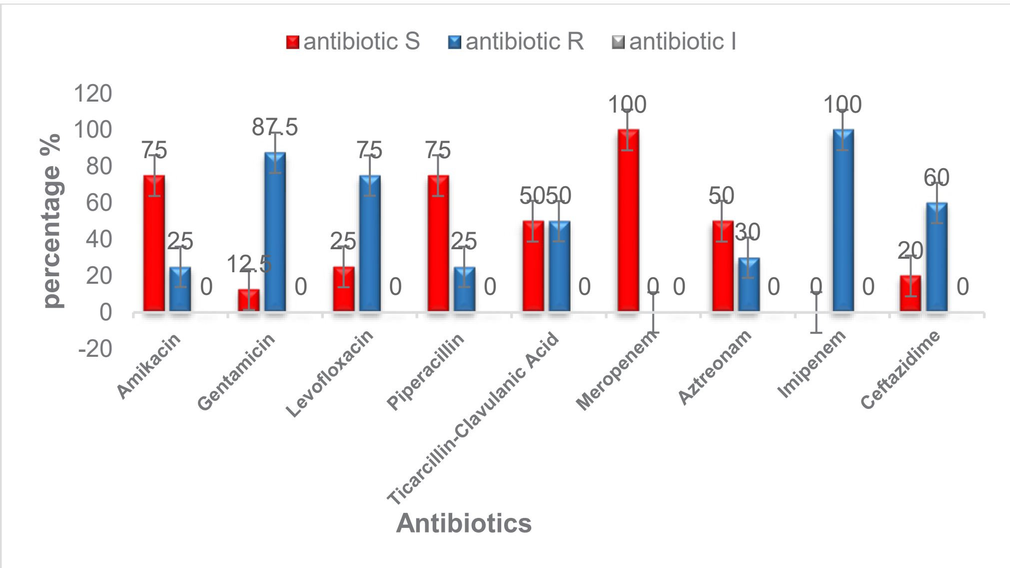

Fig. 9. Antimicrobial susceptibility test for *P. aeruginosa.*

may, in fact, be a result of the wide-scale use of these last-resort antibiotics in Babylon Province hospitals.

In contrast to piperacillin, which showed 76% resistance and just 24% susceptibility, cefepime displayed an equal distribution with 50% resistance and 50% susceptibility. Confirming the multidrug-resistant traits of this pathogen, 29.24% of *P.aeruginosa* isolates from burn victims showed resistance to three or more drugs [44]. In the Iraqi context, *P.aeruginosa* accounted for 27% of isolates from burn patients, and the emergence of multidrug-resistant strains makes continuous monitoring of resistance patterns vitally important [45].

Overall, there is a substantial and wide-scale resistance to almost all classes of antibiotics, which classifies most of these isolates as MDR *P. aeruginosa*. Furthermore, it is known that *P.aeruginosa* causes difficult-to-treat infections that have a naturally low susceptibility to many antibiotics and often require combination therapy [46]. Our results also put forth the urgent need for the implementation of strict antimicrobial stewardship programs and regular resistance pattern surveillance, and, at the same time, we must look into alternative therapeutic approaches—which are reported in the present study—to fight against MDR *P.aeruginosa* in burn units.

Using biosynthesized magnesium oxide nanoparticles (MgO NPs) derived from dragon plant extracts, researchers investigated the inhibitory effect on *P.aeruginosa*, a clinically important Gram-negative bacterium isolated from burn wounds. The concentrations of nanoparticles varied from 250 to 1000 µg/ml. Experimental results indicated that the size of the inhibition zones increased with increasing nanoparticle concentration. The diameters of the inhibition zones ranged from 15 mm in *P.aeruginosa* at 1000 µg/ml (Fig. 10) to 11 mm at 500 µg/ml. However, no bacterial inhibition was observed at 250 µg/ml, indicating that this concentration falls below the minimum inhibitory threshold required to suppress bacterial growth. The antibacterial potential may be first shown by agar well diffusion; however, it does not give quantitative inhibitory concentrations like MIC and MBC. So, to learn more about the therapeutic possibilities of the produced nanoparticles, more research is needed to establish the minimal inhibitory and bactericidal doses, but by comparing the antibiotic susceptibility profile of the isolates indirectly with the antibacterial activity of MgO NPs, their potential as alternative agents against MDR strains may be highlighted.

In terms of what magnesium oxide nanoparticles do at a cellular level, there are many theories. Also, it has been put forth that the large surface area of nanoparticles, which in turn increases their point of contact with biological systems as compared to larger bulk particles, is what gives them their great antibacterial action [47]. Furthermore, the play of the nanoparticles doesn't only include interaction with the membrane surface but may also include disruption of outer membrane structure, interference with key cell functions, and the production of reactive oxygen species, which, in turn, cause oxidative damage to what is inside the bacteria [48, 49]. In 2023, [50] reported that the phytochemical capping agents present

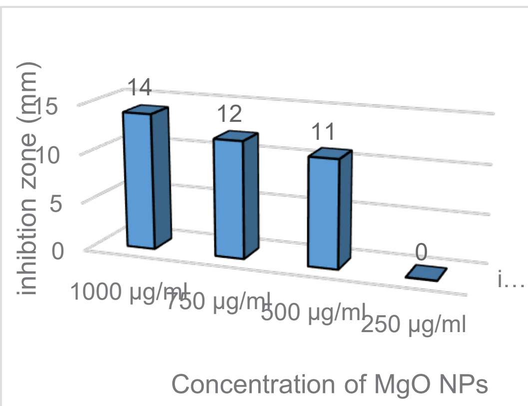

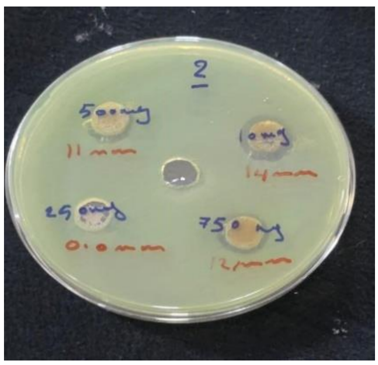

Fig. 10. Antibacterial activity of biosynthesized MgO NPs at different concentrations.

in the plant extract used for biosynthesis exert a synergistic effect, which we observe in the antibacterial action. Furthermore, the extract has a wide range of bioactive, like phenolics and flavonoids, which they note also play very independent roles in displaying antimicrobial activity against gram-negative bacteria. Future studies must include suitable positive controls in addition to the negative control to substantiate the observed antibacterial effects, given that the existing experimental design is devoid of control groups.

In the area of biomedicine, see that many antibacterial drugs and delivery systems that are put forth use nanotechnology, which is a focus of a great deal of research [51]. Also, see that biosynthesized MgO NPs do, in fact, put forward effective results against bacteria. Also, it is put forth in other studies that there is a minimum effective concentration that must be achieved before green-synthesized metal oxide nano particles see to have a large bacterial inhibiting effect [52, 53].

In fact, all nanomaterials that enter the bloodstream do in fact interact with red blood cells; find that evaluation of the biocompatibility of biosynthesized nanoparticles is a very important step in the assessment of their biological safety. Per the American Society for Testing and Materials (ASTM), a hemolysis rate of less than 5% is what is put forward as a mark of hemocompatibility and biological acceptability [54].

This study's findings showed that the biosynthesized MgO NPs did not exhibit any hemolytic activity at any of the doses tested (0.12, 0.25, 0.5, and 1 mg/mL), with a hemolysis percentage of 0% across the board (Fig. 11). Highlighting the therapeutic relevance of confirming non-hemolytic behavior prior to any biomedical application, these findings are especially noteworthy because hemoglobin release into plasma can cause serious adverse health outcomes such as anemia, pulmonary hypertension, and renal toxicity [55].

In this study, a range of non-hemolytic concentrations is reported, including those of the full spectrum of concentrations that produce the antimicrobial, antioxidant, and other biological effects seen from these nanoparticles, which in turn confirms that we may achieve the therapeutic benefits of these particles without at the same time damaging red blood cells.

Based on these findings, the biosynthesized MgO NPs made from plant extract (a green synthesis process) are a harmless and biocompatible nanomaterial. By doing away with the necessity for potentially harmful chemical reagents, this method encourages more sustainable and ecologically friendly methods of manufacturing. Adopting such environmentally friendly nanotechnology is therefore in line with the overarching aim of responsible production and consumption, which is in line with the twelfth sustainable development goal.

Among the limitations observed in this study that should be considered in future research are the need to determine the minimum inhibitory concentration (MIC) and the minimum lethal

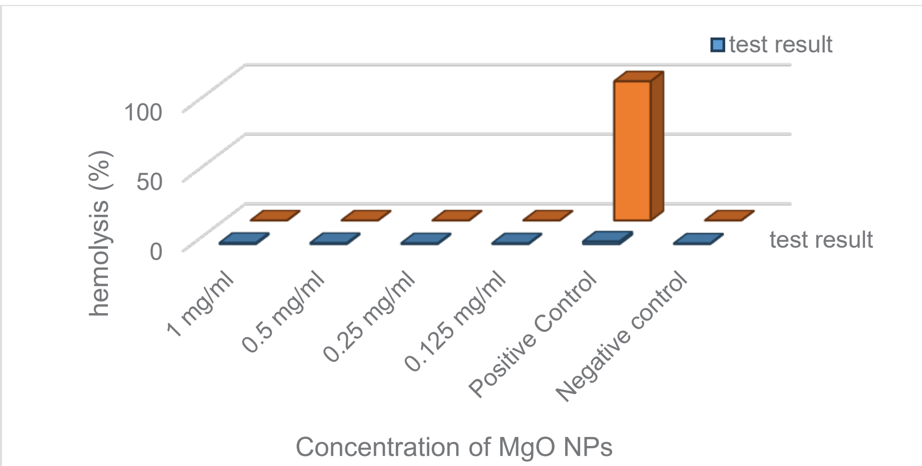

Fig. 11. The inhibition zone diameters of Dragon fruit peels treated with MgO NPs against *Pseudomonas*.

concentration (MBC), to include comprehensive control groups in antibiotic assays, and to conduct advanced statistical analysis. Furthermore, there is a need to focus on the quantitative evaluation of antibiotics and their in vivo validation.

CONCLUSION

The research found that the peel of the dragon fruit (*Hylocereus polyrhizus*) may be used to make magnesium oxide nanoparticles in an efficient and eco-friendly way. Inhibiting and stabilizing nanosynthesis may be possible, according to preliminary chemical experiments, due to bioactive components in plant extracts.

Many characterization methods verified the synthesis of nanoparticles with improved biological activity due to their nanoscale size and desired morphological and structural features. The synthetic particles prevented the growth of burn patients' multidrug-resistant Pseudomonas aeruginosa bacteria and showed antioxidant activity that depended on concentration, suggesting they may replace bacteria.

Hemocompatibility testing supported the particles' biosafety and therapeutic potential by demonstrating no hemolytic impact at the tested levels. This study's nanoparticles could help treat burn infections in medical applications. To validate treatment effectiveness and understand their processes, the study proposes molecular and in vivo investigations.

ACKNOWLEDGMENTS

Our deepest gratitude goes out to the biology department, College of Science for Women at Babylon University, for all of their help with this project.

CONFLICT OF INTEREST

The authors declare that there is no conflict of interests regarding the publication of this manuscript.

REFERENCES

1. Abushouk AI, Negida A, Ahmed H, Abdel-Daim MM. Neuroprotective mechanisms of plant extracts against MPTP induced neurotoxicity: Future applications in Parkinson's disease. Biomedicine and Pharmacotherapy. 2017;85:635-645.
2. Moharil MP, Gangurde SS, Ingle KP, Khelurkar VC, Jadhav PV, Ghorade RB, et al. Molecular characterization of metal homeostasis related gene orthologs in nutri-rich foxtail millet accessions. AGRICULTURE UPDATE. 2017;12(Special-1):409-420.
3. Markiewicz-Gospodarek A, Kozioł M, Tobiasz M, Baj J, Radzikowska-Büchner E, Przekora A. Burn Wound Healing: Clinical Complications, Medical Care, Treatment, and Dressing Types: The Current State of Knowledge for Clinical Practice. International Journal of Environmental Research and Public Health. 2022;19(3):1338.
4. Yakupu A, Zhang J, Dong W, Song F, Dong J, Lu S. The epidemiological characteristic and trends of burns globally. BMC Public Health. 2022;22(1).
5. Skowrońska W, Bazylko A. The Potential of Medicinal Plants and Natural Products in the Treatment of Burns and Sunburn—A Review. Pharmaceutics. 2023;15(2):633.
6. Ruillé M, Dorey E, Dorel M. Estimation of nitrogen uptake dynamics in banana with two simple indicators of biomass. Fruits. 2023;78(3):1-10.
7. Paśko P, Galanty A, Zagrodzki P, Ku YG, Luksirikul P, Weisz M, et al. Bioactivity and cytotoxicity of different species of pitaya fruits – A comparative study with advanced chemometric analysis. Food Bioscience. 2021;40:100888.
8. Bordoh PK, Ali A, Dickinson M, Siddiqui Y. Antimicrobial effect of rhizome and medicinal herb extract in controlling postharvest anthracnose of dragon fruit and their possible phytotoxicity. Scientia Horticulturae. 2020;265:109249.
9. Joshi M, Prabhakar B. Phytoconstituents and pharmaco-therapeutic benefits of pitaya: A wonder fruit. J Food Biochem. 2020;44(7).
10. Huang Y, Brennan MA, Kasapis S, Richardson SJ, Brennan CS. Maturation Process, Nutritional Profile, Bioactivities and Utilisation in Food Products of Red Pitaya Fruits: A Review. Foods. 2021;10(11):2862.
11. Poolsup N, Suksomboon N, Paw NJ. Effect of dragon fruit on glycemic control in prediabetes and type 2 diabetes: A systematic review and meta-analysis. PLoS One. 2017;12(9):e0184577.
12. Seth S, kaba L, Ahirwar S, jain p, Pagare M, Sinha R, et al. Characterization of dragon fruit (Hylocereus undatus) antioxidative components to explore their utility as natural food additive. Egyptian Journal of Food Science. 2021;0(0):0-0.
13. Khan ST, Musarrat J, Al-Khedhairy AA. Countering drug resistance, infectious diseases, and sepsis using metal and metal oxides nanoparticles: Current status. Colloids Surf B Biointerfaces. 2016;146:70-83.
14. Negut I, Grumezescu V, Grumezescu AM. Treatment Strategies for Infected Wounds. Molecules. 2018;23(9):2392.
15. dos Santos Gomes D, de Sousa Victor R, de Sousa BV, de Araújo Neves G, de Lima Santana LN, Menezes RR. Ceramic Nanofiber Materials for Wound Healing and Bone Regeneration: A Brief Review. Materials. 2022;15(11):3909.
16. Hu H, Xu F-J. Rational design and latest advances of polysaccharide-based hydrogels for wound healing. Biomaterials Science. 2020;8(8):2084-2101.
17. Kushwaha RK, Deepa HN, Karkera P, Jayashree S. Antibacterial Activity of Silver Nanoparticles Synthesized Using Syzygium aromaticum, Cinnamonum tamala, Cinnamonum cassia Plant Extract. Journal of Pharmaceutical Research International. 2021:20-31.
18. Adedayo O, Anderson WA, Moo-Young M, Snieckus V, Patil PA, Kolawole DO. Phytochemistry and Antibacterial Activity of Senna alata Flower. Pharm Biol. 2001;39(6):408-412.
19. Adesegun SA, Ayoola GA, Coker HA, Adepoju-Bello AA, Obaweya K, Ezennia EC, et al. Phytochemical Screening and

Antioxidant Activities of Some Selected Medicinal Plants Used for Malaria Therapy in Southwestern Nigeria. Tropical Journal of Pharmaceutical Research. 2008;7(3).
20. Hasan BJ, Al-Mutar HA-aH, Taher JK, Hussain SO. Effects of Adding Natural Honey to Semen Extender on Ram Epididymal Sperm Quality. World's Veterinary Journal. 2025;15(1):109-116.
21. Paterson. Phytochemical Methods. A Guide to Modern Techniques of Plant Analysis. Plant Pathol. 1999;48(1):146-146.
22. Anyasor GN, Onajobi FD, Osilesi O, Adebawo OO. Phytochemical Constituents in Hexane Fraction of Costus afer Ker Gawl. Stem. Vedic Research International Phytomedicine. 2014;2(3):66.
23. Ganguly S, Das S, Dastidar SG. A study on structural ,morphological and chemical composition of zinc sulphide nanoparticles synthesized by a simple chemical technique. International Journal of Scientific Research. 2012;2(7):472-473.
24. Hiesgen R, Wehl I, Helmly S, Haug A, Schulze M, Bauder A, et al. Atomic force microscopy and infrared analysis of aging processes of polymer electrolyte membrane fuel cell components. J Electroanal Chem. 2011;662(1):240-250.
25. Arnab A, Goyal A, Middha S. Evaluation of the DPPH radical scavenging activity, total phenols and antioxidant activities in Indian wild Bambusa vulgaris "Vittata" methanolic leaf extract. Journal of Natural Pharmaceuticals. 2010;1(1):40.
26. KaragÖZ A, Acar S, KÖRkoca H. Characterization of Klebsiella isolates by matrix-assisted laser desorption/ionization time-of-flight mass spectrometry (MALDI-TOF MS) and determination of antimicrobial resistance with VITEK 2 advanced expert system (AES). TURKISH JOURNAL OF MEDICAL SCIENCES. 2015;45:1335-1344.
27. Laloy J, Minet V, Alpan L, Mullier F, Beken S, Toussaint O, et al. Impact of Silver Nanoparticles on Haemolysis, Platelet Function and Coagulation. Nanobiomedicine. 2014;1.
28. Study of protopectinase activity on fruits peels for release of pectin using ruthenium red dye. International Journal of Recent Trends in Engineering and Research. 2017;3(11):13-17.
29. Ibrahim SRM, Mohamed GA, Khedr AIM, Zayed MF, El-Kholy AA-ES. Genus Hylocereus: Beneficial phytochemicals, nutritional importance, and biological relevance-A review. J Food Biochem. 2018;42(2):e12491.
30. Saenjum C, Pattananandecha T, Nakagawa K. Antioxidative and Anti-Inflammatory Phytochemicals and Related Stable Paramagnetic Species in Different Parts of Dragon Fruit. Molecules. 2021;26(12):3565.
31. . BIOLINK (Jurnal Biologi Lingkungan Industri Kesehatan). 2026;12(2).
32. Felhi S, Daoud A, Hajlaoui H, Mnafgui K, Gharsallah N, Kadri A. Solvent extraction effects on phytochemical constituents profiles, antioxidant and antimicrobial activities and functional group analysis of Ecballium elaterium seeds and peels fruits. Food Science and Technology. 2017;37(3):483-492.
33. Silva CPD, Sousa MSB, Siguemoto ÉS, Soares RAM, Arêas JAG. Chemical composition and antioxidant activity of jatobá-do-cerrado (Hymenaea stigonocarpa Mart.) flour. Food Science and Technology (Campinas). 2014;34(3):597-603.
34. Naipospos M, Idris M, Rahmadina R. PENAPISAN FITOKIMIA DAN PENENTUAN KADAR FLAVONOID EKSTRAK DAUN SEMBUNG [BLUMEA BALSAMIFERA (L.) DC] DI DESA HASANG DAN DESA SIMANGALAM KECAMATAN KUALUH SELATAN KABUPATEN LABUHANBATU UTARA. KLOROFIL: Jurnal Ilmu Biologi dan Terapan. 2022;6(2):54.
35. Oyshi SA, Jahan RA, Aktar F, Sultan MZ, Chowdhury AA, Chowdhury JA, et al. Preparation and evaluation of the biosynthetic procedure of iron oxide and magnesium oxide nanoparticles using Hylocereus undatus fruit peel extract and their anticancer properties. RSC Advances. 2025;15(19):15366-15374.
36. Suresh J, Yuvakkumar R, Sundrarajan M, Hong SI. Green Synthesis of Magnesium Oxide Nanoparticles. Advanced Materials Research. 2014;952:141-144.
37. Makhlouf SA, Kassem MA, Abdel-Rahim MA. Particle size-dependent electrical properties of nanocrystalline NiO. Journal of Materials Science. 2009;44(13):3438-3444.
38. Santhoshkumar J, Kumar SV, Rajeshkumar S. Synthesis of zinc oxide nanoparticles using plant leaf extract against urinary tract infection pathogen. Resource-Efficient Technologies. 2017;3(4):459-465.
39. Esquivel P, Stintzing FC, Carle R. Phenolic Compound Profiles and their Corresponding Antioxidant Capacity of Purple Pitaya (Hylocereus sp.) Genotypes. Zeitschrift für Naturforschung C. 2007;62(9-10):636-644.
40. Estahbanati HK, Kashani PP, Ghanaatpisheh F. Frequency of Pseudomonas aeruginosa serotypes in burn wound infections and their resistance to antibiotics. Burns. 2002;28(4):340-348.
41. Alaghehbandan R, MacKay Rossignol A, Rastegar Lari A. Pediatric burn injuries in Tehran, Iran. Burns. 2001;27(2):115-118.
42. Messadi AA, Lamia T, Kamel B, Salima O, Monia M, Saida BR. Association between antibiotic use and changes in susceptibility patterns of Pseudomonas aeruginosa in an intensive care burn unit: A 5-year study, 2000–2004. Burns. 2008;34(8):1098-1102.
43. Ghasemian S, Karami-Zarandi M, Heidari H, Khoshnood S, Kouhsari E, Ghafourian S, et al. Molecular characterizations of antibiotic resistance, biofilm formation, and virulence determinants of Pseudomonas aeruginosa isolated from burn wound infection. J Clin Lab Anal. 2023;37(4).
44. Ullah F, Malik SA, Ahmed J. Antimicrobial susceptibility and ESBL prevalence in Pseudomonas aeruginosa isolated from burn patients in the North West of Pakistan. Burns. 2009;35(7):1020-1025.
45. Othman N, Babakir-Mina M, Noori CK, Rashid PY. Pseudomonas aeruginosa infection in burn patients in Sulaimaniyah, Iraq: risk factors and antibiotic resistance rates. The Journal of Infection in Developing Countries. 2014;8(11):1498-1502.
46. Naji EN, Ali AA, Hamzah BF. The Bactericidal Effect of CO_2 Laser on Pseudomonas aeruginosa Isolated from Wound and Burn Infections, In-Vitro. Baghdad Science Journal. 2015;12(3):485-495.
47. Science and Technology Against Microbial Pathogens2011 2011/07: WORLD SCIENTIFIC.
48. Patil SV, Borase HP, Patil CD, Salunke BK. Biosynthesis of Silver Nanoparticles Using Latex from Few Euphorbian Plants and Their Antimicrobial Potential. Applied Biochemistry and Biotechnology. 2012;167(4):776-790.
49. Saleh GM. Green Synthesis Concept of Nanoparticles From Environmental Bacteria and Their Effects on Pathogenic Bacteria. Iraqi Journal of Science. 2020:1289-1297.

50. Rotti RB, Sunitha DV, Manjunath R, Roy A, Mayegowda SB, Gnanaprakash AP, et al. Green synthesis of MgO nanoparticles and its antibacterial properties. Frontiers in Chemistry. 2023;11.
51. Ojha S, Sett A, Bora U. Green synthesis of silver nanoparticles by Ricinus communis var. carmencita leaf extract and its antibacterial study. Advances in Natural Sciences: Nanoscience and Nanotechnology. 2017;8(3):035009.
52. Kim JS, Kuk E, Yu KN, Kim J-H, Park SJ, Lee HJ, et al. Antimicrobial effects of silver nanoparticles. Nanomed Nanotechnol Biol Med. 2007;3(1):95-101.
53. Sondi I, Salopek-Sondi B. Silver nanoparticles as antimicrobial agent: a case study on E. coli as a model for Gram-negative bacteria. Journal of Colloid and Interface Science. 2004;275(1):177-182.
54. Luna-Vázquez-Gómez R, Arellano-García ME, García-Ramos JC, Radilla-Chávez P, Salas-Vargas DS, Casillas-Figueroa F, et al. Hemolysis of Human Erythrocytes by Argovit™ AgNPs from Healthy and Diabetic Donors: An In Vitro Study. Materials. 2021;14(11):2792.
55. Rother RP, Bell L, Hillmen P, Gladwin MT. The Clinical Sequelae of Intravascular Hemolysis and Extracellular Plasma Hemoglobin. JAMA. 2005;293(13):1653.